Smart Electrochemical Morphine Sensor Using poly(3,4-ethylene-dioxythiophene)/Gold-nanoparticles Composite in Presence of Surfactant

Nada F. Atta[*], *Ahmed Galal, Ekram H. El-Ads,*

Department of Chemistry, Faculty of Science, Cairo University, 12613 Giza, Egypt
[*]E-mail: nada_fah1@yahoo.com

The amount of morphine (MO) in the blood and urine must be controlled and maintained within safe ranges. Some chromatographic and spectrophotometric techniques are sensitive to MO but they suffer from several drawbacks. Thus, it is required to construct a novel simple, fast, cheap and highly sensitive sensor for MO. An electrochemical MO sensor in presence of sodium dodecyl sulfate (SDS) was proposed by utilizing gold nanoparticles over poly(3,4-ethylene-dioxythiophene) modified gold electrode (Au/PEDOT-Au$_{nano}$…SDS). Enhanced electrocatalytic activity towards MO oxidation was achieved at Au/PEDOT-Au$_{nano}$…SDS compared to Au/PEDOT and Au/PEDOT-Au$_{nano}$. The MO concentration could be measured at Au/PEDOT-Au$_{nano}$…SDS in the linear range of 2 μM to 18 μM with correlation coefficient of 0.9983 and very low detection limit of 0.428 nM. Furthermore, the simultaneous and selective determinations of MO, ascorbic acid (AA) and uric acid (UA), MO and dopamine (DA) and MO and atropine (AT) proved excellent with high sensitivity and reproducibility. Moreover, the validity of this sensor in tablets and real urine samples resulted in achieving very low detection limit of MO with excellent recovery results.

1. INTRODUCTION

Opiates are considered the favorable drugs for the short-treatment of post-surgical pains as well as for long-term treatment of severe pains in cancer patients. Morphine (MO), the most effective painkiller, is considered the reference by which analgesics are assessed. Moreover, MO is the most studied and most commonly used intravenous drug for Patient-Controlled Analgesia. However, large or repeated doses can induce prolonged sedation, nausea, vomiting, apathy, reduced physical activity, dysphoria, constipation, hypotension and respiratory depression, which further can lead to disruption in

the central nervous system, toxication and death [1-3]. Therefore, it is very necessary for the biomedical applications to detect and maintain the MO concentrations in the blood and urine within safe ranges [4, 5]. To date, there are many techniques for detecting MO including high-performance liquid chromatography [6], gas chromatography–mass spectroscopy [7], thin layer chromatography, surface plasmon resonance [8], radioimmunoassay [9], enzyme-linked immunosorbent assay, sequential injection analysis [10], chemiluminescence [11] and spectrophotometric methods [12]. However, these techniques are sensitive to MO concentrations, there are several disadvantages of these methods. They are very expensive, complicated and restricted by the search for a suitable antibody and enzyme that react with MO. As well, they are also very time-consuming, inconvenient in MO detection in clinical analysis and delicate instruments are required [8]. Therefore, it is required to develop a simple, fast and highly sensitive method for MO detection.

Electrochemical methods have received much interest due to their higher selectivity, lower detection limit, lower cost and faster operation than other reported methods [13-15]. Recently, many electrochemical sensors for direct determination of MO were constructed. Stationary platinum, graphite [16] or planar glassy carbon electrodes [17, 18], gold microelectrode [19], graphene nanosheets [20], electrodeposited Prussian blue thin film [21], ordered mesoporous carbon [22], cobalt hexacyanoferrate modified electrodes [23], ZnO/carbon nanotubes nanocomposite/ionic liquid [24], gold nanoparticles–ferrocene modified carbon paste electrodes [25], PEDOT modified electrodes were used [8, 15, 26].

Poly(3,4-ethylenedioxythiophene) (PEDOT) is very promising in the design of electrochemical sensors. It has proved to adhere strongly on most electrode materials, present good stability in aqueous electrolytes, show high conductivity in its oxidized state, have biocompatibility with biological media and resist fouling by the oxidation products [27-29]. On the other hand, it has been reported that nanomaterials modified electrodes particularly; gold nanoparticles, can accelerate electron transfer rate, enhance conductivity of electrodes and have good biocompatibility in biomolecules detection owing to their small dimensional size, good conductivity and excellent catalytic activity [30-32]. Furthermore, pristine conducting polymers can be modified by the inclusion of metal functionalities particularly; noble metal nanoparticles, inside the polymeric matrix in order to further improve the performances of the resulting composite material [33-35]. Gold nanoparticles can be grown inside the PEDOT matrix by chemical routes [36, 37] or by simultaneous electrodeposition of polymer along with metal nanoparticles [38-41] or by electrochemical deposition of gold nanoparticles on the PEDOT prepared by spin coating method [42] or on the electropolymerized PEDOT [43].

Surfactants have proven effective in the electroanalysis of biological compounds and drugs [26, 28, 30] as they have high impact in the enhancement of the electrode/solution interface properties [44-46]. Different modified electrodes were used for determination of DA [28, 45-47], MO [15] and terazosin [44] in presence of SDS and tryptophan in presence of sodium dodecylbenzene sulfonate [30].

The aim of the present study is to construct a novel electrochemical MO sensor which is free from the drawbacks of the other reported methods. This electrochemical sensor is simple, fast, cheap, selective and highly sensitive for MO. It was constructed by the electrodeposition of gold nanoparticles into the electropolymerized PEDOT film over the surface of gold (Au) electrode. Au/PEDOT-

Au$_{nano}$…SDS was used for the first time for the sensitive determination of MO and it is not reported elsewhere in the literature. The voltammetric response of Au/PEDOT-Au$_{nano}$…SDS is highly selective toward MO compared to Au/PEDOT and Au/PEDOT-Au$_{nano}$. On the other hand, the proposed sensor is prepared in simple steps with cheap and simple reagents and no pretreatment needed before the measurements. This gives the sensor more advantages over other methods used in the literature. In addition, the anti-interference ability of the proposed sensor was confirmed via the simultaneous determinations of MO and DA, MO and AT and MO, AA and UA.

2. EXPERIMENTAL

2.1. Chemicals and reagents

All chemicals were used as received without further purification. 3,4-Ethylene dioxy-thiophene (EDOT), tetrabutylammonium hexafluorophosphate (TBAHFP), acetonitrile ([HPLC] grade), dopamine (DA), uric acid (UA), ascorbic acid (AA), sodium dodecyl sulfate (SDS) and hydrogen tetrachloroaurate (HAuCl$_4$) were supplied by Aldrich Chem. Co. (Milwaukee, WI. USA). Morphine (MO) sulfate was supplied from Forensic Chemistry Laboratory, Medico Legal Department, Ministry of Justice, Cairo, Egypt. Atropine (AT) sulfate was supplied by Novartis Pharma (Egypt). Aqueous solutions were prepared using double distilled water. Britton–Robinson (B-R) buffer (pH 2–9, 0.12 M) are prepared from 0.12 M boric acid, 0.12 M acetic acid and 0.12 M orthophosphoric acid; the pH was adjusted by 0.2 M NaOH.

2.2. Electrochemical cells and equipments

Electrochemical polymerization and characterization were carried out with a three-electrode/one compartment glass cell. The working electrode was gold disc (diameter: 1 mm). The auxiliary electrode was in the form of 6.0 cm platinum wire. All the potentials in the electrochemical studies were referenced to Ag/AgCl (4 M KCl saturated with AgCl) electrode. Working electrode was polished using alumina (2µm)/water slurry until no visible scratches were observed. Prior to immersion in the cell, the electrode surface was thoroughly rinsed with distilled water and dried. All experiments were performed at 25 °C ± 0.2 °C. The electrosynthesis of the PEDOT film, gold nanoparticles and their electrochemical characterization were performed using a BAS-100B electrochemical analyzer (Bioanalytical Systems, BAS, West Lafayette, USA).

EIS was performed using a Gamry-750 instrument and a lock-in-amplifier that are connected to a personal computer. The data analysis was provided with the instrument and applied non-linear least square fitting with Levenberg-Marquardt algorithm. All impedance experiments were recorded between 0.1 Hz and 100 kHz with an excitation signal of 10 mV amplitude. The measurements were performed under potentiostatic control at different applied potentials which were decided from the cyclic voltammogram recorded for the modified electrode. Quanta FEG 250 instrument was used to obtain the scanning electron micrographs (SEM) of the different films.

2.3. Electropolymerization of EDOT

The polymer film was electrochemically formed by applying a constant potential (1400 mV) to the working Au electrode for 30 s (Bulk Electrolysis, BE). The thickness of the film was controlled by the amount of charge consumed during the electro-polymerization (assuming 100% efficiency during the electrochemical conversion). The synthesis solution consisted of 0.01 M monomer (3,4-EDOT), and 0.01 M supporting electrolyte (TBAHFP) dissolved in acetonitrile ([HPLC] grade).

2.4. Preparation of Au/PEDOT-Au$_{nano}$ composite electrodes

Briefly, a polymer film is prepared and washed with doubly distilled water. This was followed by the electrochemical deposition of gold nanoparticles from a solution containing 6 mM HAuCl$_4$ prepared in 0.1 M KNO$_3$ (prepared in doubly distilled water and deaerated by bubbling with nitrogen). The potential applied between the working Au/PEDOT electrode and the reference Ag/AgCl (4 M KCl saturated with AgCl) electrode is held constant at -400 mV (Bulk electrolysis, BE) for 400 s. The surface coverage (Γ) of gold nanoparticles was approximately 4.4×10^{-6} mol/cm^2 (estimated from the quantity of charge used in the electrodeposition process). This electrode is denoted as Au/PEDOT-Au$_{nano}$. Further modification is done by the successive additions of 10 µL of 0.1 M SDS (prepared in distilled water) to the morphine solution (0.5 mM MO/ B-R (pH 7.40, 0.12 M)) from 0 up to 200 µL (increments add 6.7×10^{-5} M SDS of each addition and the total concentration of SDS after 20 additions is 1.3×10^{-3} M) and the electrode is denoted as Au/PEDOT-Au$_{nano}$…SDS. After each addition, stirring takes place for 5 min. then holds for 1 min. before running the experiment.

2.5. Analysis of urine

The utilization of the proposed method in real sample analysis was also investigated by direct analysis of MO in human urine samples. MO was dissolved in urine to make a stock solution with 0.5 mM concentration. Standard additions were carried out from the MO stock solution in 15 mL of B-R buffer (pH 7.40, 0.12 M) containing 200 µL SDS.

2.6. Application on tablets

Tablets of the studied drug were used as performed. Tablets dissolved to form 1.3 mM stock solution. Standard additions were carried out from the MO stock solution in 15 mL of B-R buffer (pH 7.40, 0.12 M) containing 200 µL SDS.

3. RESULTS AND DISCUSSION

*3.1. Electrochemistry of MO at different modified electrodes*

The voltammetric behavior of 0.5 mM MO/ B-R buffer (pH 7.40, 0.12 M) was examined at bare Au (I), Au/PEDOT (II), Au/PEDOT-Au$_{nano}$ (III) and Au/PEDOT-Au$_{nano}$…SDS (IV) electrodes

(Figure 1) at scan rate 50 mV s^{-1}. The catalytic activity of the modified electrode toward MO oxidation was confirmed from the values of oxidation peak current and potential. The oxidation current of MO increases from 1.20 μA at bare Au to 2.68 μA, 4.66 μA and 11.3 μA at Au/PEDOT, Au/PEDOT-Au$_{nano}$ and Au/PEDOT-Au$_{nano}$...SDS electrodes, respectively. Moreover, the anodic peak of MO shifted to 423 mV, 462 mV and 403 mV at Au/PEDOT, Au/PEDOT-Au$_{nano}$ and Au/PEDOT-Au$_{nano}$...SDS, respectively compared to 493 mV at bare Au electrode. Therefore, the voltammetric response of Au/PEDOT-Au$_{nano}$…SDS is highly selective toward MO compared to Au/PEDOT and Au/PEDOT-Au$_{nano}$. The oxidation peak of MO at Au/PEDOT-Au$_{nano}$…SDS is attributed to the oxidation of the phenolic group (−OH) at the 3-position leading to the formation of pseudomorphine as the main product involving one-electron transfer (Equation 1) [15, 22]. As the structure of pseudomorphine possesses two phenolic groups, its further oxidation is possible occurring at the same potential as MO. Thus, the peak at 403 mV is attributed to the oxidation of the phenolic groups in MO and pseudomorphine. Similar voltammetric peaks were observed at bare Au, Au/PEDOT and Au/PEDOT-Au$_{nano}$ with lower current response.


(1)
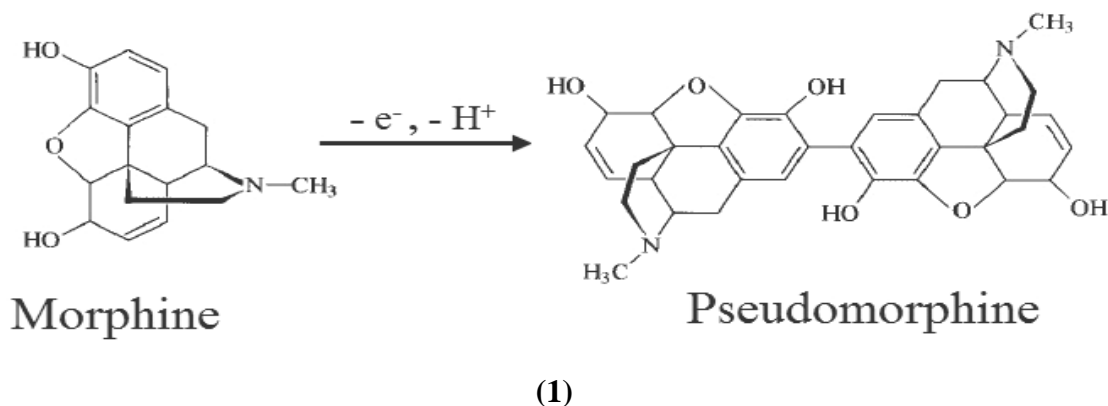
The proposed sensor, Au/PEDOT-Au$_{nano}$…SDS, indicates the synergism between the conductive PEDOT, gold nanoparticles and SDS for the selective and sensitive determination of MO. It combines the properties of PEDOT to reduce the oxidation potential with the attractive electrocatalytic properties of gold nanoparticles and SDS to promote a faster electron transfer rate. In more details, the catalytic activity of the proposed sensor can be explained in terms of the surface morphology. The PEDOT film contains a distribution of hydrophobic (reduced) and hydrophilic (oxidized) regions and the hydrophobic MO^{+} cations prefer to interact with the more hydrophobic regions. Also, the PEDOT film has a rich electron cloud that acts as an electron mediator. SEM image of PEDOT film (Figure 2 A) indicates a globular morphology and a rough surface due to the Au substrate. The increase in oxidation current of MO at Au/PEDOT-Au$_{nano}$ is attributed to the catalytic effect of gold nanoparticles acting as a promoter to accelerate the electron transfer rate. The SEM of PEDOT-Au$_{nano}$ (Figure 2 B) shows that metallic nanoparticles are located at different elevations over the PEDOT film exploring a large surface area. The conductivity level of PEDOT-Au$_{nano}$ film is influenced by the aggregates of SDS that accumulates onto the surface and helps the attraction of MO (selectively) to the electrode surface. PEDOT-Au$_{nano}$ film becomes spongy due to the presence of anionic tailing structure of SDS (Figure 2 C). SDS is an anionic surfactant with hydrophobic tail

consisting of 12 carbon atoms and hydrophilic head consisting of sulfate group. The suggested mechanism for the aggregation of surfactants on the modified electrode surface in the form of bilayers, cylinder, or surface micelles (in the case of relatively higher concentrations added of SDS) could explain the increase in the current in the presence of surfactant (Figure 2 D). The electron transfer process will take place when the electroactive species approaches the vicinity of the electrode surface. The charge transfer is achieved via the approach of the analyte to the electrode surface within the space of one to two head groups of adsorbed surfactant moieties.
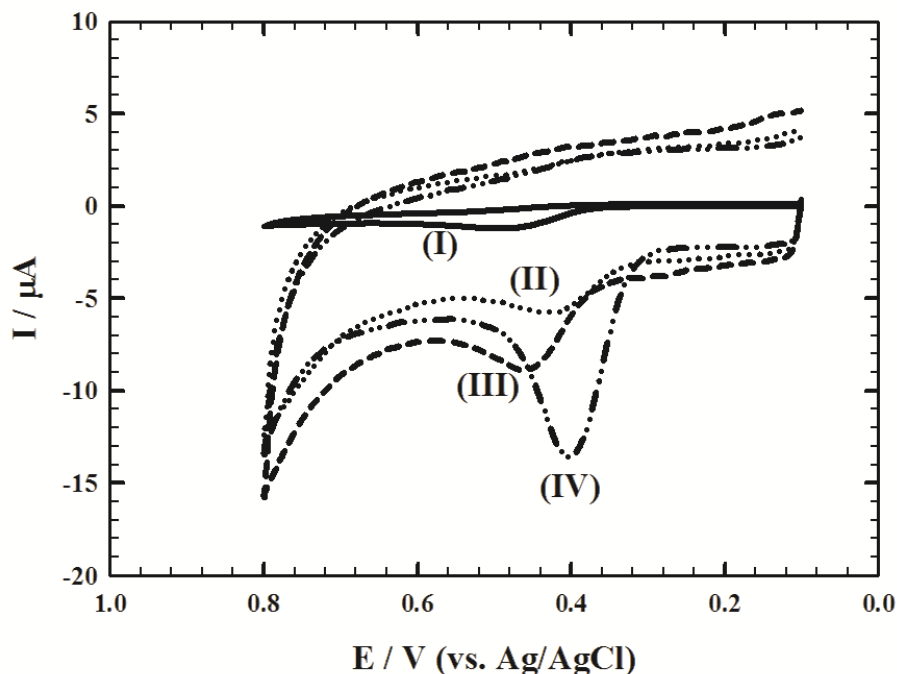
Figure 1. CVs of 0.5 mM MO/ B-R (pH 7.40, 0.12 M) at: (I) bare Au, (II) Au/PEDOT, (III) Au/PEDOT-Au$_{nano}$, and (IV) Au/PEDOT-Au$_{nano}$…SDS modified electrodes, scan rate 50 mV s^{-1}.
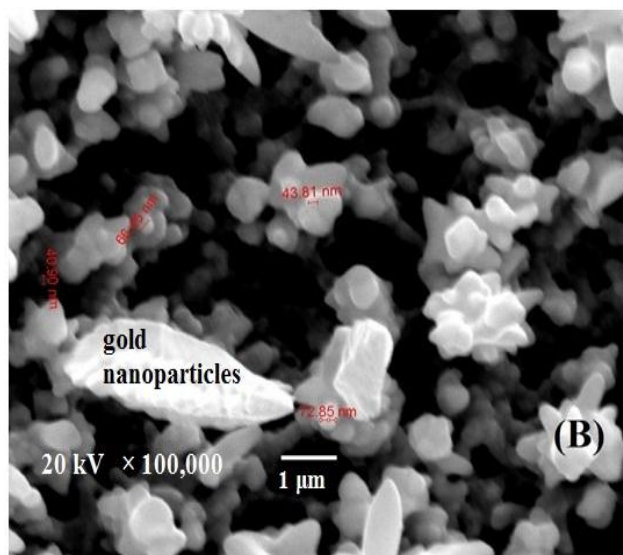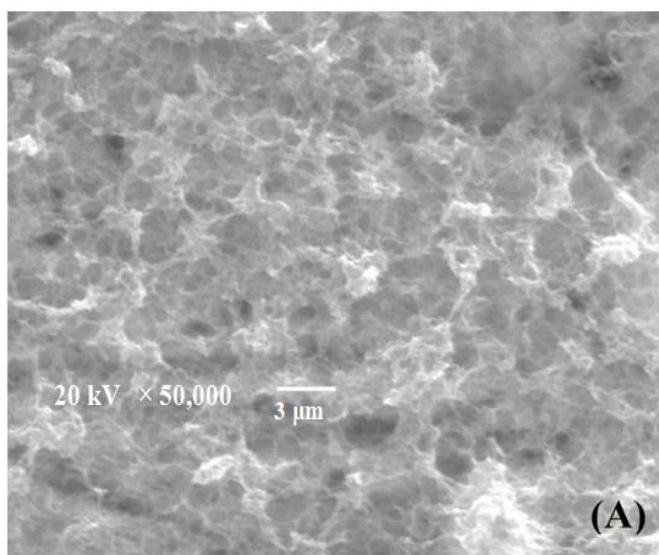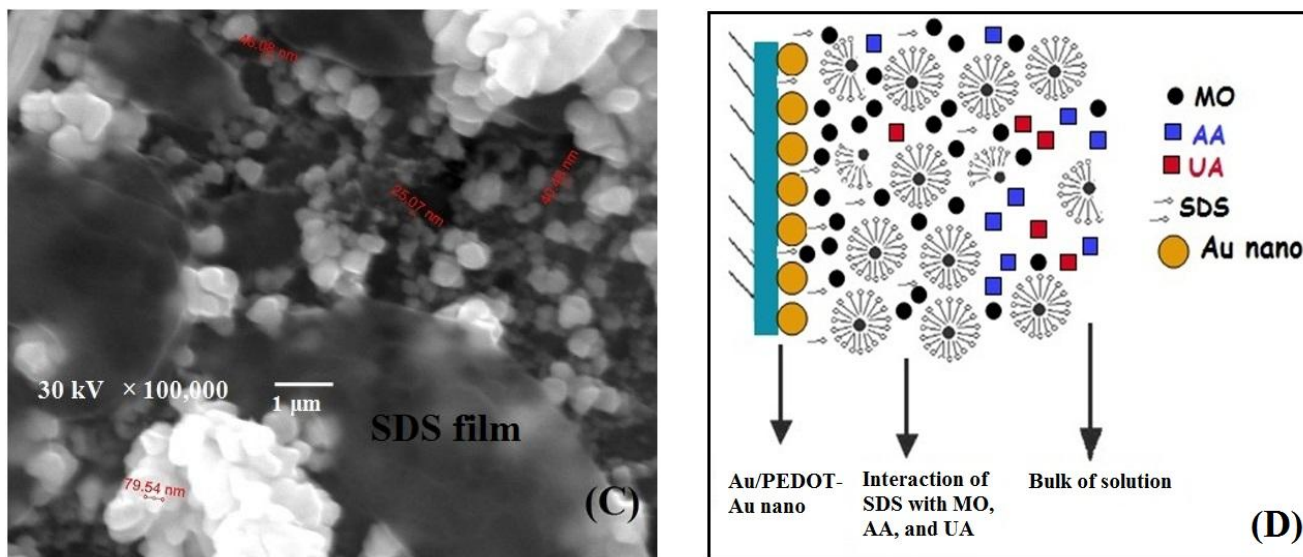
Figure 2. SEM images of: Au/PEDOT (**A**), Au/PEDOT-Au$_{nano}$ (**B**), and Au/PEDOT-Au$_{nano}$...SDS (**C**) electrodes. (**D**) Schematic model of Au/PEDOT-Au$_{nano}$ modified electrode in presence of SDS, MO, AA and UA.

The formation of ion-pair of the charged surfactant and drug adhering to the electrode surface through the lipophilic parts in both moieties is a possible mechanism [28, 44]. Thus, the addition of SDS enhances the preconcentration/accumulation of MO$^+$ cations, accelerates the rate of electron transfer due to the electrostatic attraction of positively charged MO (pK$_a$ of phenolic group of MO= 9.4) [15] with the anionic surfactant SDS and enhances the MO current signal at the Au/PEDOT-Au$_{nano}$ modified electrode. Thus, this promising electrochemical sensor is used for the sensitive and selective determination of MO in presence of AA, and UA.

3.2. Scan rate effect

The peak currents (I$_p$) of 0.5 mM MO at Au/PEDOT-Au$_{nano}$…SDS were varied with change of scan rate (Figure 3). In details, varying scan rate from 10 to 150 mV s^{-1} resulted in a positive shift of the oxidation peak potential and an increase of peak current for MO. A plot of the anodic peak current values versus the square root of the scan rate results in a straight-line relationship indicating a diffusion-controlled process (inset of Figure 3) [14, 22]. The dependence of the anodic peak current (I$_p$ /A) on the scan rate has been used for the estimation of the "apparent" diffusion coefficient D$_{app}$ of MO. D$_{app}$ (cm^2 s^{-1}) values were calculated from Randles Sevcik equation (Equations 2, 3) [28] and for the oxidized species [O]:

$$I_p = 0.4463 \, (F^3 / RT)^{1/2} \, n^{3/2} \, \nu^{1/2} \, D^{1/2} \, A \, C \qquad (2)$$

For T = 298 K (temperature at which the experiments were conducted), the equality holds true:

$$I_p = (2.687 \times 10^5) \, n^{3/2} \, \nu^{1/2} \, D^{1/2} \, A \, C \qquad (3)$$

where the constant has unit (i.e. 2.687×10^5 C mol^{-1} V$^{-1/2}$).

In these equations (2, 3): I_p is the peak current (A), n is the is the number of electrons exchanged in oxidation (n =1), v is the scan rate (V s^{-1}), F is Faraday's constant (96485 C mol^{-1}), C is the analyte concentration (0.5 mM), A is the geometrical electrode area $= 7.854 \times 10^{-3}$ cm^2, R is the universal gas constant (8.314 J mol^{-1} K^{-1}), T is the absolute temperature (K) and D is the electroactive species diffusion coefficient (cm^2 s^{-1}) [28, 33]. It is important to notice that the apparent surface area used in the calculations does not take into account the surface roughness, which is inherent characteristic for polymer films and gold nanoparticles. The roughness factor calculated from atomic force microscopy measurements is 1.52, 1.91 and 1.92 for Au/PEDOT, Au/PEDOT-Au$_{nano}$ and Au/PEDOT-Au$_{nano}$…SDS, respectively indicating larger surface area upon modification of PEDOT film with gold nanoparticles and SDS. D_{app} values for MO are 2.57×10^{-5}, 1.28×10^{-4}, 3.89×10^{-4} and 2.29×10^{-3} cm^2 s^{-1} at bare Au, Au/PEDOT, Au/PEDOT-Au$_{nano}$ and Au/PEDOT-Au$_{nano}$…SDS. The D_{app} values indicated that the diffusion component of the charge transfer is highly enhanced at Au/PEDOT-Au$_{nano}$…SDS compared to other modified electrodes indicating the role of gold nanoparticles and SDS in accelerating the rate of electron transfer [15, 28].
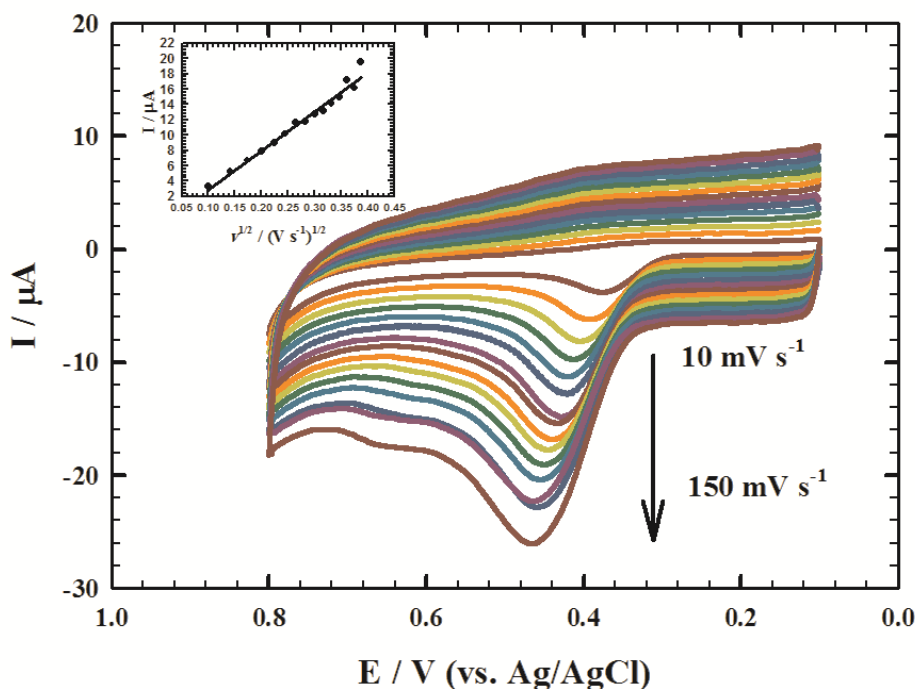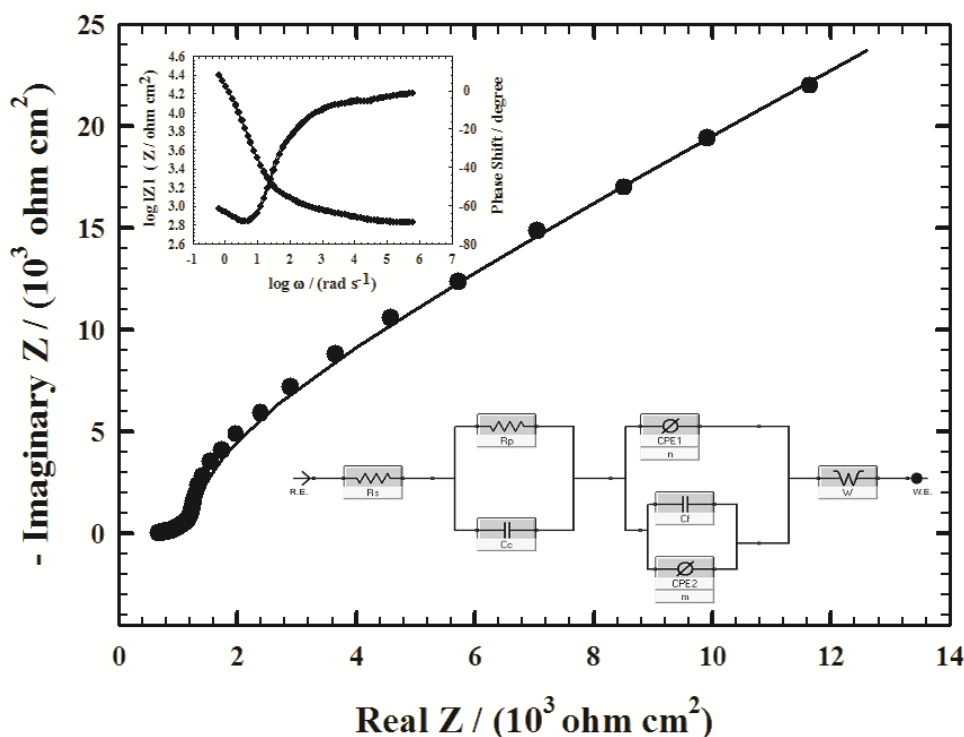

Figure 3. CVs of 0.5 mM MO/ B-R (pH 7.40, 0.12 M) at Au/PEDOT- Au$_{nano}$…SDS modified electrode at different scan rates (10 mV s^{-1} - 150 mV s^{-1}), the inset; linear relationship of the anodic peak current (I_p /A) vs. the square root of the scan rate ($v^{1/2}$) /(V s^{-1})$^{1/2}$ in the range of 10 mV s^{-1} - 150 mV s^{-1}, (I_p /A = (− 2.30×10^{-6}) + 5.13×10^{-5} $v^{1/2}$ /(V s^{-1})$^{1/2}$, R^2 = 0.9747).

3.3. Electrochemical impedance spectroscopy (EIS)

The nature of MO interaction at Au/PEDOT-Au$_{nano}$…SDS was examined using EIS. EIS data were obtained at AC frequency varying between 0.1 Hz and 100 kHz with an applied potential (410 mV) in the region corresponding to the electrolytic oxidation of 0.5 mM MO/ B-R (pH 7.40, 0.12 M).

Figure 4 and the inset show a typical impedance spectrum presented in the form of Nyquist and Bode plots of MO at Au/PEDOT-Au$_{nano}$…SDS, respectively. The inset of Figure 4 shows the equivalent circuit, where R_s is the solution resistance and R_p is the polarization resistance. Capacitors in EIS experiments do not behave ideally; instead they act like a constant phase element (CPE). Therefore, CPE$_1$ and CPE$_2$ are constant phase elements and n, and m are their corresponding exponents (n is nearly one, and m is less than one). C_c and C_f represent the capacitance of the double layer [33]. Diffusion can create an impedance known as the Warburg impedance W. Table (1) lists the best fitting values calculated from the equivalent circuit for the impedance data of Figure 4. The impedance spectra include a semicircle portion at the higher frequencies and a linear portion at the lower frequencies describing the electron-transfer limiting and the diffusion-limiting electrochemical processes, respectively. The semicircle diameter equals the interfacial charge transfer resistance R_{ct} which controls the electron transfer kinetics of the redox probe at the electrode interface. The diameter of the semicircle part in Figure 4 diminishes markedly implying a low charge transfer resistance R_{ct} of the redox probe due to the selective interaction between SDS and MO resulting in the facilitation of the charge transfer. The values of the capacitive component indicating the conducting character of the modified surface due to ionic adsorption at the electrode surface and the charge transfer process.

Figure 4. Nyquist plot of Au/PEDOT-Au$_{nano}$…SDS in 0.5 mM MO/ B-R(pH 7.40, 0.12 M) at the oxidation potential (410 mV), and the insets, the equivalent circuit used in the fit procedure of the impedance spectra and the typical impedance spectrum presented in the form of Bode plot where ω is the angular frequency (rad s^{-1}). (symbols and solid lines represent the experimental measurements and the computer fitting of impedance spectra, respectively), frequency range: 0.1–100000 Hz.

3.4. Effect of solution pH on electrochemistry of MO

Furthermore, pH value of the supporting electrolyte (B-R buffer) is an important parameter in determining the performance of electrochemical sensors. The effect of changing the pH of the supporting electrolyte on the electrochemical response of MO was studied. It is clear that changing the pH (pH 2.60, 4.30, 7.40 and 9.08) of the supporting electrolyte altered both the peak potentials and peak currents of MO indicating that the electrocatalytic oxidation of MO at the Au/PEDOT-Au_{nano}…SDS is a pH-dependent reaction and protonation/deprotonation is taking part in the charge transfer process. The anodic peak potential shifted negatively with the increase in the solution pH due to the facilitation of the deprotonation involved in the oxidation process at higher pH values.

Figure 5 shows the linear relationship between the anodic peak potential and the solution pH value over the pH range 2.60 to 9.08 with a slope of -0.056 V/pH units which is close to the theoretical value of -0.059 V/pH. This indicated that the overall process is proton dependent with an equal number of protons and electrons involved in MO oxidation [15, 18]. As the MO oxidation is one-electron process, the number of protons involved was also predicted to be one indicating a $1e^-/1H^+$ process [8, 22]. The inset of Figure 5 shows the relationship between the solution pH values and the anodic peak currents of MO at Au/PEDOT-Au_{nano} electrode in absence (1) and in presence (2) of SDS; the anodic peak current of MO decreased as pH increased. This is related to the differences in the surface properties of the electrode in absence and presence of SDS and the variation of electrostatic interaction between MO and the anionic SDS at different pHs. Moreover, the decrease of the peak current in alkaline medium might be due to the decomposition of MO at higher pH values. At physiological pH, MO, a weak base with the pK_a of about 8.08, is primarily ionized with pK_a values of 8.4 and 9.4 corresponding to the tertiary amine and the phenolic groups, respectively [15, 18].

Table 1. EIS fitting data corresponding to Figure 4.

Rs/ $10^2\ \Omega cm^2$	Cc/ $10^{-7}\ Fcm^{-2}$	Rp/ $10^1\ \Omega cm^2$	W/ $10^3\ \Omega\ s^{-1/2}$	CPE1/ $10^4\ Fcm^{-2}$	n	Cf/ $10^{-6}\ Fcm^{-2}$	CPE2/ $10^4\ Fcm^{-2}$	m
6.628	6.701	8.321	6.003	8.895	0.9880	3.031	1.511	0.7149

3.5. Determination of MO at Au/PEDOT-Au_{nano}…SDS

The voltammetric behavior of MO was examined using linear sweep voltammetry (LSV) with scan rate 50 mV s^{-1}. The inset of Figure 6 shows typical LSVs of standard additions of 0.5 mM MO/ B-R (pH 7.40, 0.12 M) to 200 µL of 0.1 M SDS in 15 mL of B-R (pH 7.40, 0.12 M). The inset shows that by increasing the concentration of MO, the anodic peak current increases which indicates that the electrochemical response of MO is apparently improved by SDS due to the enhanced accumulation of protonated MO via electrostatic interaction with negatively charged SDS at Au/PEDOT-Au_{nano} [15]. Figure 6 shows the calibration curve of the anodic peak current values in the linear range of 2 µM to 18 µM with the regression equation of (I_p /A = (1.5913×10^{-7}) + 3.506×10^{-8} [MO]/µM and from 20 µM to

140 µM MO (Fig. not shown) with the regression equation of (I_p /A = ($4.2377×10^{-7}$) + $2.2047×10^{-8}$ [MO]/µM, with correlation coefficients of 0.9983 and 0.9988, sensitivities of 0.03506 µA/µM and 0.02205 µA/µM, detection limits of 0.428 nM and 2.72 nM and quantification limits of 1.43 nM and 9.07 nM, respectively. The detection limit (D L) and quantification limit (Q L) were calculated from the equations: D L= 3 s /b, and Q L= 10 s /b, respectively, where s is the standard deviation and b is the slope of the calibration curve.
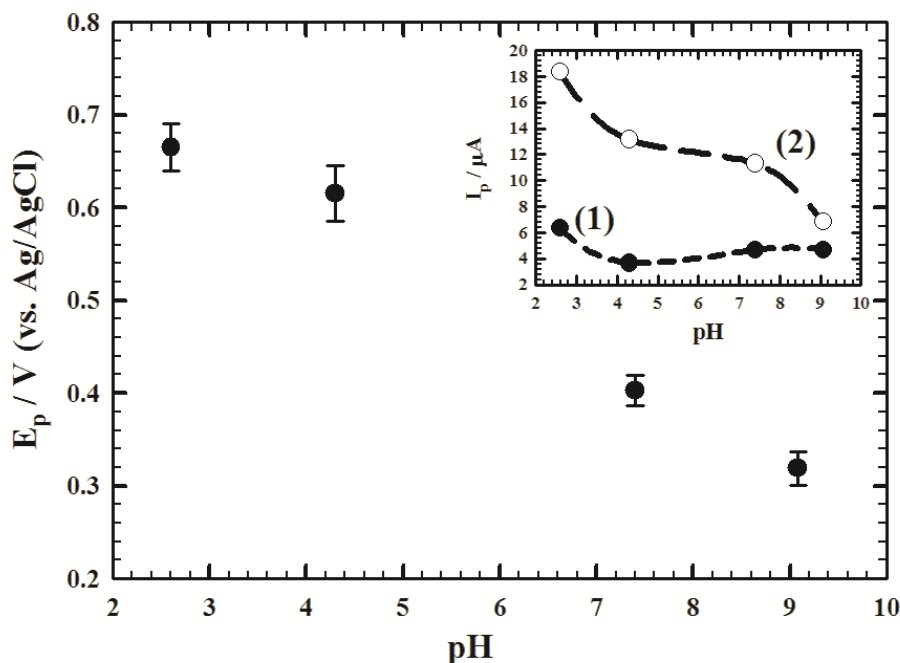
Figure 5. The dependence of the anodic peak potential (E_p / V) of MO on pH value of the solution at Au/PEDOT-Au_{nano}…SDS modified electrode, (E_p / V = 0.8289 + (- 0.05618) pH, R^2 = 0.9856), and the inset; the dependence of the anodic peak current (I_p / µA) of MO on pH value of the solution at Au/PEDOT-Au_{nano} electrode in absence **(1)** and in presence **(2)** of SDS.

Table 2 shows the comparison for the determination of MO at Au/PEDOT-Au_{nano}…SDS with various modified electrodes based in literature reports [8, 14, 15, 18]. The proposed MO sensor showed good sensing performance in terms of limit of detection and sensitivity. It also showed extra advantages; short time, low cost for the analysis and no pretreatment needed before the measurement. Atta et al have constructed Pt/PEDOT…SDS as MO sensor and the detection limit was 46 nM [15]. Much lower detection limit (0.428 nM) was obtained at Au/PEDOT-Au_{nano}…SDS compared to Pt/PEDOT…SDS indicating the role of gold nanoparticles as a mediator to enhance the electron transfer rate.

3.6. Determination of MO in spiked urine samples

It is very necessary to monitor and maintain the MO concentration in blood and urine within safe ranges. Validation of the proposed electrochemical sensor was evaluated by performing recovery tests for MO in spiked urine samples [22]. MO was dissolved in urine to make a stock solution with

0.5 mM concentration. Typical LSVs of standard additions of 0.5 mM MO in urine to 200 µL of 0.1 M SDS in 15 mL of B-R (pH 7.40, 0.12 M) showed that the oxidation peak current increased with addition of MO (Figure not shown) [15]. The detection limits of MO in urine in the linear range of 20 µM to 140 µM and 2 µM to 18 µM were 5.83 nM and 1.27 nM, respectively. Much lower detection limit (1.27 nM) for MO in urine was obtained at Au/PEDOT-Au$_{nano}$…SDS compared to 50 nM at Pt/PEDOT…SDS [15] indicating the higher catalytic activity of the proposed sensor.

Five different concentrations on the calibration curve are chosen to be repeated to evaluate the accuracy and precision of the proposed method (Table 3). The recovery of the spiked samples ranged from 99.4% to 101.9% and the results are acceptable indicating that the present procedures are free from interferences of the urine sample matrix [15, 22]. The results strongly proved that MO can be selectively and sensitively determined at Au/PEDOT-Au$_{nano}$ electrode in urine sample in presence of SDS. This sensor showed good reproducibility, high stability, enhanced sensitivity, much lower detection limit and anti-interference ability [15, 18].
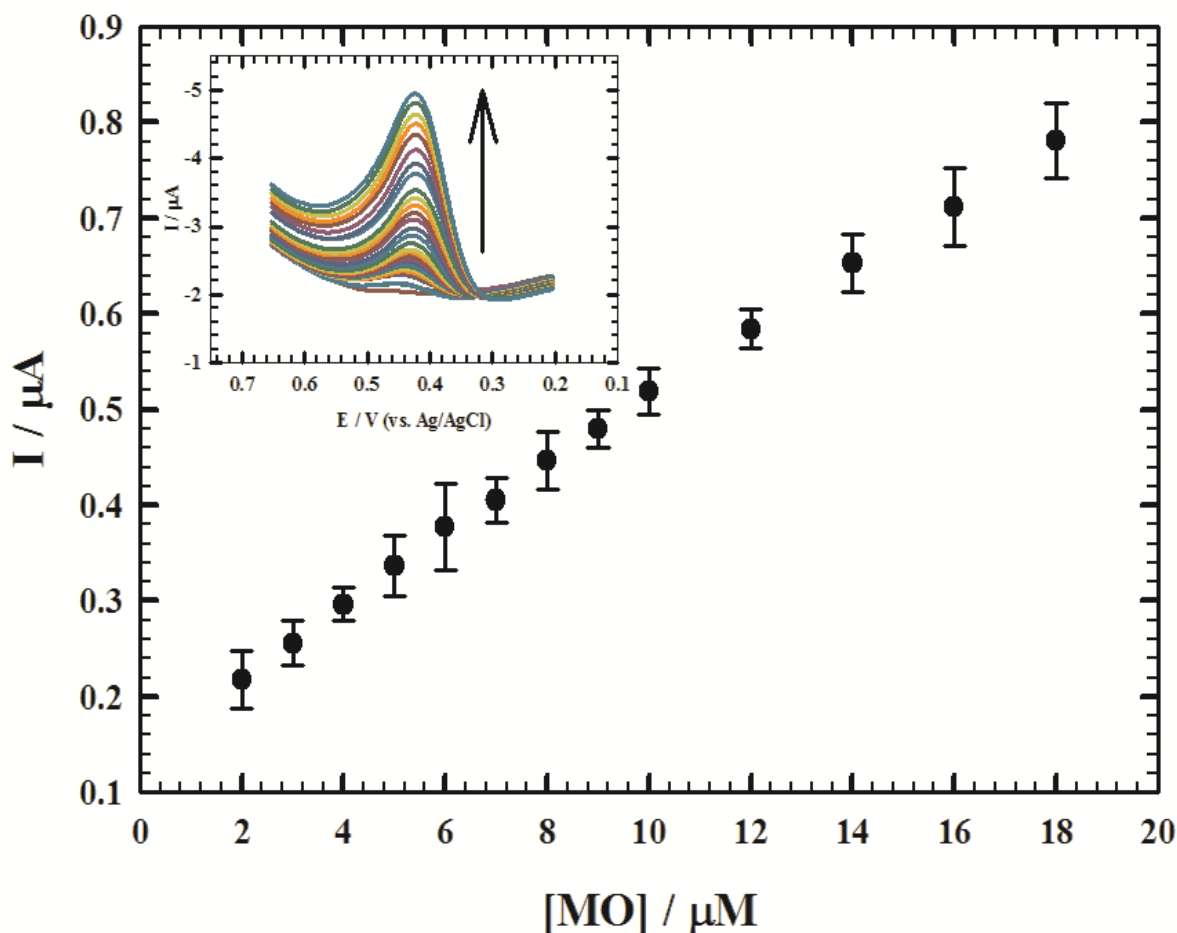
Figure 6. Calibration curve for MO for concentrations from (2 µM to 18 µM), (I_p /A = (1.5913×10^{-7}) + 3.506×10^{-8} c /µM, slope = 0.03506 (+/- 2×10^{-5}) µA/µM and intercept = 0.159129 (+/- 5×10^{-6}) µA, and R^2 = 0.9983), scan rate 50 mV s^{-1}. The inst shows LSVs of 15 ml of B-R (pH 7.40, 0.12 M) at Au/PEDOT-Au$_{nano}$…SDS modified electrode in different concentrations of MO (2 µM -140 µM).

Table 2. Comparison for determination of MO at various modified electrodes based in literature reports.

Electrode	LDR (µM)	Sensitivity (µA/µM)	LOD (nM)	Reference
Pt/ PEDOT…SDS	0.3-16	NR	46	15
ITO/ PB	$(0.09\text{-}1.0)\times10^3$	16.8	0.1×10^6	21
GCE/ OMC	0.1-20	1.74	10	22
ITO/ MIP-PEDOT	$(0.1\text{–}1)\times10^3$	0.0917	0.2×10^6	8
PGCE	4-18	0.0715	0.2×10^3	18
Pd-Al/ PB	2-50	0.0780	0.73×10^3	14
GNFMCPE	1-180	NR	3.5	25
Au/ PEDOT/Au$_{nano}$…SDS	2-18	0.0351	0.428	This work

Note. LDR, linear dynamic range; LOD, limit of detection; NR, not reported; Pt, platinum electrode; ITO, indium tin oxide; PB, Prussian blue; GCE, glassy carbon electrode; OMC, ordered mesoporous carbon; MIP-PEDOT, a molecularly imprinted polymer; PGCE, electrochemically pretreated glassy carbon electrode; Pd-Al, palladized aluminum electrode; GNFMCPE, carbon paste electrode with ferrocene/gold nanoparticles.

Table 3. Evaluation of the accuracy and precision of the proposed method for the determination of MO in urine sample.

Sample	Concentration of MO added (µM)	Concentration of found MO (µM) [a]	Recovery (%)	Standard deviation × 10^{-8}	Standard error × 10^{-8}
1	5.00	5.096	101.9	2.99	1.34
2	16.0	16.1	100.8	2.37	1.06
3	25.0	25.02	100.1	1.73	0.775
4	50.0	49.7	99.4	3.15	1.41
5	110	109.8	99.8	4.55	2.03

[a] Average of five determinations.

3.7. Applications on MO Tablets

The determination of MO in its pharmaceutical formulation (10 mg/tablet) without the necessity for any extraction steps was performed. One tablet of MO sulfate was dissolved in B-R buffer solution (pH 7.40, 0.12 M) with a start concentration of 1.3 mM. Standard successive additions of 1.3 mM of MO were added to 15 mL of B-R buffer solution (pH 7.40, 0.12 M) containing 200 µL SDS. The effect of changing the concentration of MO in presence of 200 µL of 0.1 M SDS in pH 7.40 was studied by LSV using Au/PEDOT-Au$_{nano}$ working electrode. The oxidation peak current for MO is linearly proportional to the concentration of the drug in the ranges of 60 µM to 200 µM and 5 µM to 50 µM with the detection limits of 5.19 nM and 0.661 nM, respectively (Table 4).

Table 4. Values of linear dynamic range (LDR) and limit of detection (LOD) of MO at Au/PEDOT-Au$_{nano}$…SDS in different tested solutions.

Tested Solution	LDR of MO (µM)	LOD of MO (nM)
MO Tablets	(5-50), (60-200)	0.661, 5.19
MO in presence of 0.5 mM DA	(1 –200)	1.52
MO in presence of 50 µM UA and 500 µM AA	(0.5- 20), (25- 380)	1.44, 6.01
MO in presence of 10 µM AT	(1 – 60), (70- 300)	1.14, 5.60

3.8. MO and neurotransmitters

MO specifically blocks nociceptive stimulation during surgery thus, the increase of plasma catecholamines occuring during surgery can be reduced by MO administration. The mechanism of MO action may have its etiology in the concurrent modulation of more than one neurotransmitter. Moreover, in invertebrates DA acts as the major molecule used in neural systems [15]. The simultaneous determination of MO in the presence of DA was examined as DA usually interferes with MO analysis in urine or blood. Good selectivity and high sensitivity are two most important requirements for the detection of MO in practical clinical applications. Figure 7 (A) shows the voltammetric response at Au/PEDOT-Au$_{nano}$ electrode in 0.5 mM MO solution containing 0.5 mM DA in presence of 200 µL SDS in B-R (pH 7.40, 0.12 M). By using Au/PEDOT-Au$_{nano}$…SDS modified electrode, two well defined oxidation peaks were obtained at +0.248 V and +0.432 V corresponding to DA and MO, respectively. This illustrates that it is possible to discriminate MO from DA with good separation in peak potential (ΔE_p = 0.184 V) and with relatively high oxidation current values.

On the other hand, the effect of increasing the concentration of MO (1 µM –200 µM) in presence of 0.5 mM DA and 200 µL SDS in B-R (pH 7.40, 0.12 M) using Au/PEDOT-Au$_{nano}$ electrode was shown in Figure 7 (B). Upon successive additions of MO, the current signal of MO oxidation

increases while DA oxidation current response was almost constant. The detection limit of MO in presence of 0.5 mM DA and 200 µL SDS in the linear range of 1 µM to 200 µM was 1.52 nM (Table 4). This low detection limit confirms that this electrode can detect MO selectively in presence of high concentration of DA with much higher sensitivity and reproducibility.

3.9. MO, ascorbic acid (AA) and uric acid (UA)

Large doses of AA have been reported to suppress withdrawal symptoms in opiate addicts and to prevent the development of tolerance to and physical dependence on MO. In addition, MO increases UA levels and AA oxidation [15]. Therefore, it is necessary to examine the electrochemical behavior of MO, UA and AA in a mixture solution. To assess the selectivity of Au/PEDOT-Au$_{nano}$...SDS modified electrode; UA and AA potential interferents were investigated in the presence of 0.5 mM MO. Cyclic voltammetry was used for the characterization of a solution containing mixture of 0.5 mM MO, 0.5 mM UA, and 0.5 mM AA in B-R (pH 7.40, 0.12 M) at Au/PEDOT-Au$_{nano}$...SDS modified electrode. As shown in Figure 8 (A), the oxidation potential peaks appeared at potentials of 0.470 V, 0.362 V and 0.017 V for MO, UA and AA, respectively at Au/PEDOT-Au$_{nano}$ electrode. The large peak potentials separation allows simultaneous determination of MO, UA and AA in their mixture. In presence of 200 µL SDS in B-R (pH 7.40, 0.12 M); a sharp well defined oxidation peak of MO appeared at 0.422 V. Moreover, the oxidation peak current for MO increased in presence of SDS, while the oxidation peaks for UA and AA disappeared. The high response for MO was observed due to the electrostatic interaction of the anionic surfactant with the protonated MO in pH 7.40, but in case of AA (pK$_a$ =4.10) and UA (pK$_a$ =5.4) electrostatic repulsion takes place as AA and UA are in their anionic forms provoking a large decrease in the peak current values (Figure 2 D). SDS forms a monolayer on Au/PEDOT-Au$_{nano}$ surface with a high density of negatively charged end directed outside the electrode which enhances the accumulation of protonated MO via electrostatic interactions and improves MO oxidation current signal while the corresponding signals for AA and UA are quenched via electrostatic repulsion. Therefore, we can determine MO selectively in the presence of AA and UA.

The effect of increasing the concentration of MO (0.5 µM –380 µM) in presence of 50 µM UA, 500 µM AA and 200 µL SDS in B-R (pH 7.40, 0.12 M) using Au/PEDOT-Au$_{nano}$ electrode was shown in Figure 8 (B). The peaks of AA and UA were suppressed and upon successive additions of MO, the current signal of MO oxidation increases. The detection limits of MO in presence of 50 µM UA, 500 µM AA and 200 µL SDS in B-R (pH 7.40, 0.12 M) in the linear range from 25 µM to 380 µM and from 0.5 µM to 20 µM were 6.01 nM and 1.44 nM, respectively (Table 4). Au/PEDOT-Au$_{nano}$...SDS can determine MO selectively in presence of high concentration of AA and UA with high sensitivity and reproducibility.
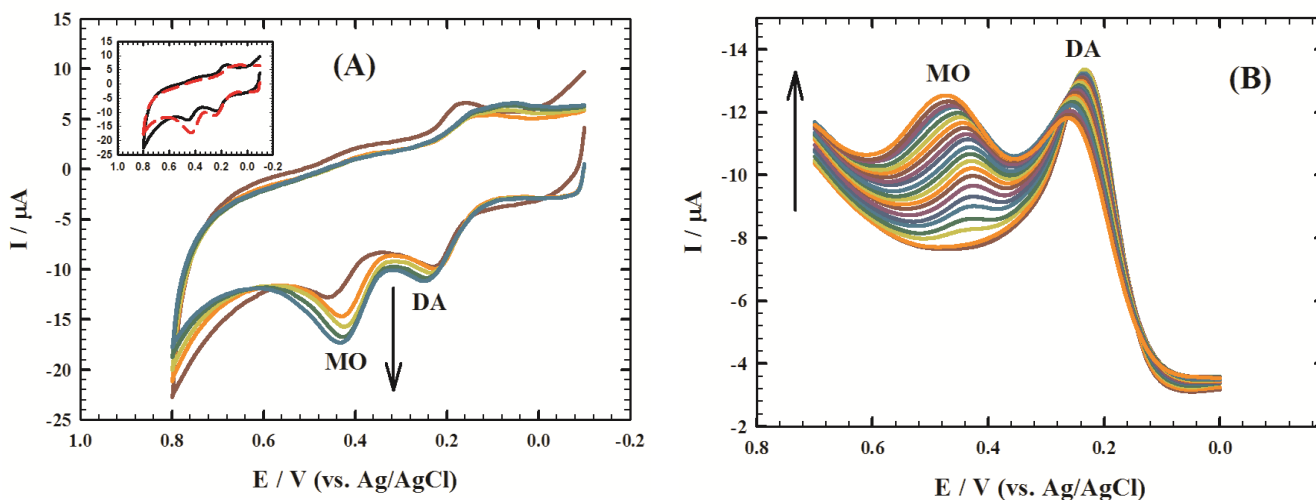
Figure 7. **(A)** CVs for equimolar solution 0.5 mM for each of MO and DA in B-R (pH 7.40, 0.12 M) at Au/PEDOT-Au$_{nano}$ modified electrode with successive additions of 0.1 M SDS (0–200 µL), inset represents the initial (in absence of SDS) and final (in presence of 200 µL SDS) CVs, scan rate 50 mV s^{-1}, **(B)** LSVs for MO of different concentrations (1 µM –200 µM) in presence of 0.5 mM DA and 200 µL SDS in B-R (pH 7.40, 0.12 M) using Au/PEDOT-Au$_{nano}$ electrode.
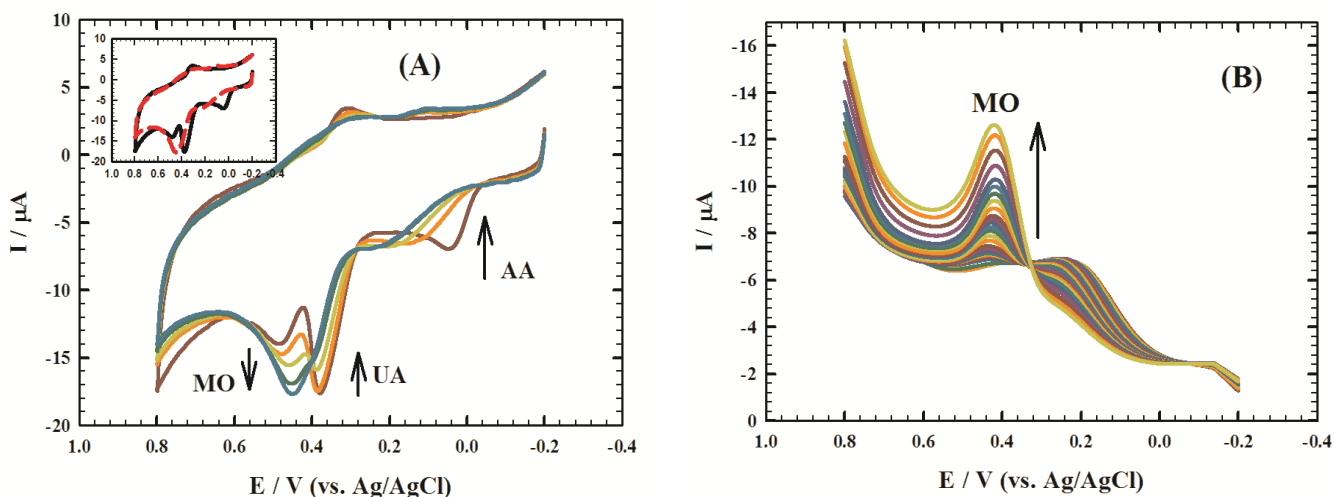

Figure 8. **(A)** CVs for equimolar solution 0.5 mM for each of MO, UA and AA in B-R (pH 7.40, 0.12 M) at Au/PEDOT-Au$_{nano}$ modified electrode with successive additions of 0.1 M SDS (0–200 µL), inset represents the initial (in absence of SDS) and final (in presence of 200 µL SDS) CVs, scan rate 50 mV s^{-1}, **(B)** LSVs for MO of different concentrations (0.5 µM–380 µM) in presence of 50 µM UA, 500 µM AA, and 200 µL SDS in B-R (pH 7.40, 0.12 M) using Au/PEDOT-Au$_{nano}$ electrode.

3.10. Simultaneous determination of MO and atropine

Atropine sulfate is an active alkaloid, naturally occurred in plants and has wide medical applications, e.g. for dilating the pupils in the ophthalmic operations, as an antispasmodic and as an antidote for poisoning of opium, eserine and muscarine. Atropine is also used in small doses in pre-

anaesthetic medication, for the treatment of cardiopathy, parkinsonism and in ophthalmic diagnosis [48]. Atropine is used in the treatment of bradycardia (an extremely low heart rate), asystole and pulseless electrical activity in cardiac arrest. This works because the main action of the vagus nerve of the parasympathetic system on the heart is to decrease heart rate. Atropine blocks this action and therefore may speed up the heart rate. Atropine can be used to reduce the effect of the poisoning by blocking muscarinic acetylcholine receptors, which would otherwise be over stimulated by excessive acetylcholine accumulation. Since MO and AT are alkaloids, a mixture of them commonly used in pre-medication in anesthesia and they play an important role in respiratory system and alveoli during surgery therefore their simultaneous determination is very important.

Figure 9 (A) shows the voltammetric response at Au/PEDOT-Au$_{nano}$ electrode in 0.5 mM MO solution containing 30 µM AT in absence (solid line) and in presence (dash line) of 200 µL SDS in B-R (pH 7.40, 0.12 M). In presence of 200 µL SDS, two well defined oxidation peaks of MO and AT appeared at 0.416 V and 0.658 V, respectively with separation (ΔE_p) more than 0.242V and the oxidation peak currents for both alkaloids increased due to the electrostatic interaction of the anionic surfactant with the protonated MO and AT in pH 7.40. This experiment studies the possibilities of simultaneous determination of the two alkaloids in the same time with good resolution. The effect of increasing the concentration of MO (1 µM – 100 µM) in presence of 10 µM AT and 200 µL SDS in B-R (pH 7.40, 0.12 M) using Au/PEDOT-Au$_{nano}$ electrode was shown in Figure 9 (B). Upon successive additions of MO, the current signal of MO oxidation increased while AT oxidation current response was almost constant. This indicates that the modified electrode can determine MO sharply in presence of AT. The detection limits of MO in presence of 10 µM AT and 200 µL SDS in B-R (pH 7.40, 0.12 M) in the linear range from 70 µM to 300 µM, and from 1 µM to 60 µM were 5.60 nM, and 1.14 nM, respectively (Table 4). This confirms that Au/PEDOT-Au$_{nano}$…SDS can determine MO selectively in presence of AT with high sensitivity and reproducibility.
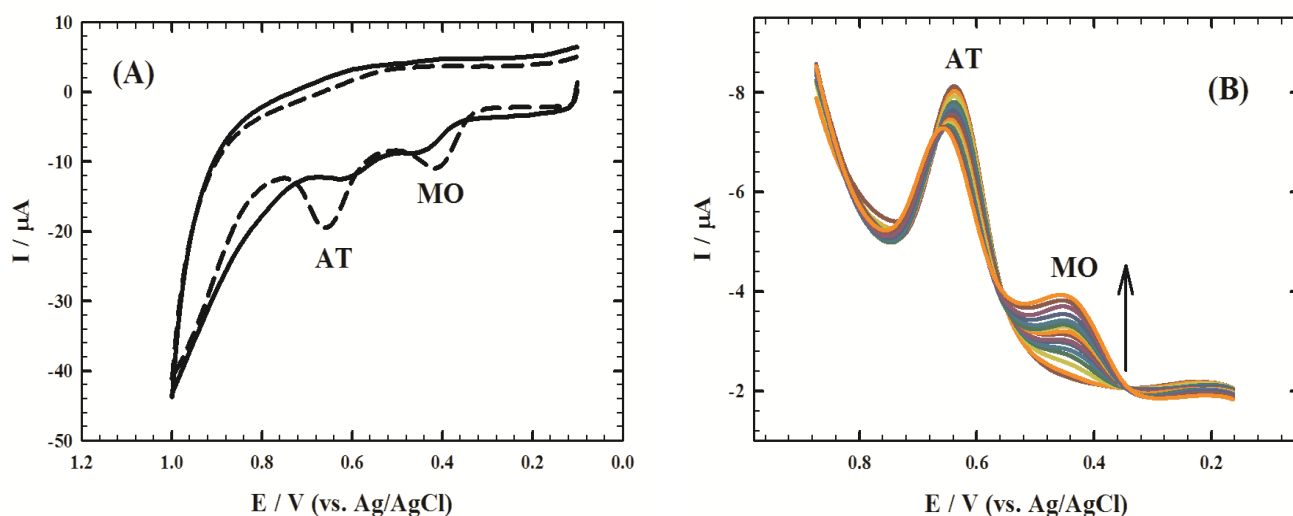
Figure 9. (A) CVs of 0.5 mmol L^{-1} MO solution containing 30 µM AT in absence (solid line) and in presence (dash line) of 200 µL SDS in B-R (pH 7.40, 0.12 M), scan rate 50 mV s^{-1}, **(B)** LSVs for MO of different concentrations (1 µM–100 µM) in presence of 10 µM AT, and 200 µL SDS in B-R (pH 7.40, 0.12 M) using Au/PEDOT/Au$_{nano}$ electrode.

3.11. Stability of the proposed sensor

The stability of Au/PEDOT-Au$_{nano}$…SDS modified electrode was examined. The CVs for 0.5 mM MO/ B-R (pH 7.40, 0.12 M) solution were recorded every 5 minutes intervals. A total of 30 runs were performed without any noticeable decrease in the film response. The anodic peak current remained relatively stable indicating that Au/PEDOT-Au$_{nano}$…SDS modified electrode has a good reproducibility and does not suffer from surface fouling during the voltammetric measurements. After measurements the electrode was kept in B-R buffer (pH 7.40, 0.12 M) in the refrigerator. The modified electrode retained 93% of its initial response up to one week of storage exhibiting longer term stability.

4. CONCLUSIONS

Au/PEDOT-Au$_{nano}$…SDS modified electrode was utilized for the electrochemical determination of MO. The proposed method showed many characteristics compared to other determination methods; simple without any sample pretreatment, cheap, fast, sensitive and selective. Enhanced electrocatalytic activity for MO oxidation was achieved at Au/PEDOT-Au$_{nano}$…SDS compared to Au/PEDOT and Au/PEDOT-Au$_{nano}$. Moreover, MO can be easily discriminated from AA and UA as common interferences in biological fluids. SDS adsorbed on the surface of Au/PEDOT-Au$_{nano}$ controls the reactions of the different charged species. Furthermore, it is possible to determine MO in presence of DA and in presence of AT using Au/PEDOT-Au$_{nano}$…SDS modified electrode. The method was sensitive enough for determination of MO in clinical preparations (human urine) and in commercial tablet under physiological conditions with good precision, accuracy, selectivity and very low detection limit. The good properties of this modified electrode will expand its application in electrochemical field for the determination of other drugs in biological fluids without any interference.

References

1. V. Santos, K.J.V. López, L.M. Santos, M. Yonamine, M.J.C. Carmona and S.R.C.J. Santos, *Clinics,* 63(3) (2008) 307.
2. P. Norouzi, M.R. Ganjali, A.A. Moosavi-movahedi and B. Larijani, *Talanta,* 73 (2007) 54.
3. N.D. Pejić, S.M. Blagojević, S.R. Anić, V.B. Vukojević, M.D. Mijatovicć and J.S. Ćirić, *Anal. Chim. Acta,* 582 (2007) 367.
4. S. Hara, S. Mochinaga, M. Fukuzawa, N. Ono and T. Kuroda, *Anal. Chim. Acta,* 387 (1999) 121.
5. Q.L. Zhang, J.J. Xu, X.Y. Li, H.Z. Lian and H.Y. Chen, *J. Pharm. Biomed. Anal.,* 43 (2007) 237.
6. Q.C. Meng, M.S. Cepeda, T. Kramer, H. Zou, D.J. Matoka and J. Farrar, *J. Chromatogr. B,* 742 (2000) 115.
7. T. Hyötyläinen, H. Keski-Hynnilä and M.L. Riekkola, *J. Chromatogr. A,* 771 (1997) 360.
8. W.M. Yeh and K.C. Ho, *Anal. Chim. Acta,* 542 (2005) 76.
9. X.X. Zhang, J. Li, J. Gao, L. Sun and W.B. Chang, *J. Chromatogr. A,* 895 (2000) 1.

10. A.M. Idris and A.O. Alnajjar, *Talanta,* 77 (2008) 522.
11. J.A.M. Pulgarìn, L.F.G. Bermejo, J.M.L. Gallego and M.N.S. Garcìa, *Talanta,* 74 (2008) 1539.
12. A. Sheibani, M.R. Shishehbore and E. Mirparizi, *Spectrochim. Acta Part A,* 77 (2010) 535.
13. A. Niazi, A. Yazdanipour and *Chin. Chem. Lett.,* 19 (2008) 465.
14. M.H. Pournaghi-Azar and A. Saadatirad, *J. Electroanal. Chem.,* 624 (2008) 293.
15. N.F. Atta, A. Galal and R.A. Ahmed, *Electroanalysis,* 23 (2011) 737.
16. B. Proksa and L. Molnàr, *Anal. Chim. Acta,* 97 (1978) 149.
17. P.H. Jordan and J.P. Hart, *Analyst,* 116 (1991) 991.
18. F. Li, J. Song, D. Gao, Q. Zhang, D. Han and L. Niu, *Talanta,* 79 (2009) 845.
19. M.R. Ganjali, P. Norouzi, R. Dinarvand, R. Farrokhi and A.A. Moosavi-movahedi, *Mater. Sci. Eng. C,* 28 (2008) 1311.
20. A. Navaee, A. Salimi and H. Teymourian, *Biosens. Bioelectron.,* 31(1) (2012) 205.
21. K.C. Ho, C.Y. Chen, H.C. Hsu, L.C. Chen, S.C. Shiesh and X.Z. Lin, *Biosens. Bioelectron.,* 20 (2004) 3.
22. F. Li, J. Song, C. Shan, D. Gao, X. Xu and L. Niu, *Biosens. Bioelectron.,* 25 (2010) 1408.
23. F. Xu, M. Gao, L. Wang, T. Zhou, L. Jin and J. Jin, *Talanta,* 58 (2002) 427.
24. E. Afsharmanesh, H. Karimi-Maleh, A. Pahlavan and J. Vahedi, *J. Mol. Liq.,* 181 (2013) 8.
25. N.F. Atta, A. Galal, A.A. Wassel and A.H. Ibrahim, Int. *J. Electrochem. Sci.,* 7 (2012) 10501.
26. K.C. Ho, W.M. Yeh, T.S. Tung and J.Y. Liao, *Anal. Chim. Acta,* 542 (2005) 90.
27. F. Sekli-Belaidi, D. Evrard and P. Gros, *Electrochem. Commun.,* 13 (2011) 423.
28. N.F. Atta, A. Galal and R.A. Ahmed, *Bioelectrochemistry,* 80 (2011) 132.
29. F. Sekli-Belaidi, P. Temple-Boyer and P. Gros, *J. Electroanal. Chem.,* 647 (2010) 159.
30. C. Li, Y. Ya and G. Zhan, *Colloids Surf. B,* 76 (2010) 340.
31. Y. Hu, Y. Song, Y. Wang and J. Di, *Thin Solid Films,* 519 (2011) 6605.
32. R.N. Goyal, V.K. Gupta, M. Oyama and N. Bachheti, *Talanta,* 72 (2007) 976.
33. N.F. Atta and M.F. El-Kady, *Sens. Actuators B,* 145 (2010) 299.
34. S. Harish, J. Mathiyarasu, K.L.N. Phani and V. Yegnaraman, *J. Appl. Electrochem.,* 38 (2008) 1583.
35. H. Guan, P. Zhou, X. Zhou and Z. He, *Talanta,* 77 (2008) 319.
36. S.V. Selvaganesh, J. Mathiyarasu, K.L.N. Phani and V. Yegnaraman, *Nanoscale Res. Lett.,* 2 (2007) 546.
37. S. Harish, J. Mathiyarasu and K.L.N. Phani, *Mater. Res. Bull,.* 44 (2009) 1828.
38. J. Mathiyarasu, S. Senthilkumar, K.L.N. Phani and V. Yegnaraman, *Mater. Lett.,* 62 (2008) 571.
39. C. Zanardi, F. Terzi, L. Pigani, A. Heras, A. Colina and J. Lopez-Palacios, *Electrochim. Acta,* 53 (2008) 3916.
40. S.S. Kumar, J. Mathiyarasu and K.L. Phani, *J. Electroanal. Chem.,* 578 (2005) 95.
41. F. Terzi, C. Zanardi, V. Martina, L. Pigani and R. Seeber, *J. Electroanal. Chem.,* 619–620 (2008) 75.
42. K.M. Manesha, P. Santhosh, A. Gopalan and K.P. Lee, *Talanta,* 75 (2008) 1307.
43. Y.P. Hsiao, W.Y. Su, J.R. Cheng and S.H. Cheng, *Electrochim. Acta,* 56 (2011) 6887.
44. N.F. Atta, S.A. Darwish, S.E. Khalil and A. Galal, *Talanta,* 72 (2007) 1438.
45. G. Alarcón-Angeles, S. Corona-Avendaño, M. Palomar-Pardavé, A. Rojas-Hernández, M. Romero-Romo and M.T. Ramírez-Silva, *Electrochim. Acta,* 53 (2008) 3013.
46. J. Zheng and X. Zhou, *Bioelectrochemistry,* 70 (2008) 408.
47. N.F. Atta, A. Galal and E.H. El-Ads, *Electrochim. Acta,* 69 (2012) 102.
48. O. Rbeida, B. Christiaens, P. Hubert, D. Lubda, K.S. Boos and J. Crommen, *J. Pharm. Biomed. Anal.,* 36 (2005) 947.